Current Biology

Domestic cat larynges can produce purring frequencies without neural input

Highlights

- The domestic cat larynx can produce purring-like sounds without neural input

- Low-frequency sounds are produced based on MyoElastic-AeroDynamic (MEAD) principles

- MEAD conflicts with the previously assumed active muscle contractions (AMC) theory

- Both AMC and MEAD mechanisms are likely frequency-entrained *in vivo*

Authors

Christian T. Herbst, Tamara Prigge, Maxime Garcia, ..., Gerald E. Weissengruber, Jan G. Svec, W. Tecumseh Fitch

Correspondence

info@christian-herbst.org (C.T.H.),
tecumseh.fitch@univie.ac.at (W.T.F.)

In brief

Cat purring has been assumed to be produced by centrally controlled cyclic contractions of intrinsic laryngeal muscles, but Herbst et al. now show that cat larynges can generate purring-like sounds via self-sustained vocal fold oscillation with no neural input. This indicates that cat purring dynamics are more complex than previously assumed.

CellPress

Current Biology

Report

Domestic cat larynges can produce purring frequencies without neural input

Christian T. Herbst,[1,2,6,*] Tamara Prigge,[3] Maxime Garcia,[4] Vit Hampala,[5] Riccardo Hofer,[1] Gerald E. Weissengruber,[3] Jan G. Svec,[5] and W. Tecumseh Fitch[1,*]

[1]Bioacoustics Laboratory, Department of Behavioral and Cognitive Biology, University of Vienna, Djerassiplatz 1, Vienna 1030, Austria
[2]Janette Ogg Voice Research Center, Shenandoah Conservatory, 1460 University Drive, Winchester, VA 22601, USA
[3]Institute of Morphology, University of Veterinary Medicine, Veterinärplatz 1, Vienna 1210, Austria
[4]Department of Livestock Sciences, Research Institute of Organic Agriculture FiBL, Ackerstrasse 113, Box 219, 5070 Frick, Switzerland
[5]Voice Research Lab, Department of Experimental Physics, Faculty of Science, Palacký University, 17. listopadu 1192/12, 779 00 Olomouc, Czechia
[6]Lead contact
*Correspondence: info@christian-herbst.org (C.T.H.), tecumseh.fitch@univie.ac.at (W.T.F.)
https://doi.org/10.1016/j.cub.2023.09.014

SUMMARY

Most mammals produce vocal sounds according to the myoelastic-aerodynamic (MEAD) principle, through self-sustaining oscillation of laryngeal tissues.[1,2] In contrast, cats have long been believed to produce their low-frequency purr vocalizations through a radically different mechanism involving active muscle contractions (AMC), where neurally driven electromyographic burst patterns (typically at 20–30 Hz) cause the intrinsic laryngeal muscles to actively modulate the respiratory airflow. Direct empirical evidence for this AMC mechanism is sparse.[3] Here, the fundamental frequency (f_o) ranges of eight domestic cats (*Felis silvestris catus*) were investigated in an excised larynx setup, to test the prediction of the AMC hypothesis that vibration should be impossible without neuromuscular activity, and thus unattainable in excised larynx setups, which are based on MEAD principles. Surprisingly, all eight excised larynges produced self-sustained oscillations at typical cat purring rates. Histological analysis of cat larynges revealed the presence of connective tissue masses, up to 4 mm in diameter, embedded in the vocal fold.[4] This vocal fold specialization appears to allow the unusually low f_o values observed in purring. While our data do not fully reject the AMC hypothesis for purring, they show that cat larynges can easily produce sounds in the purr regime with fundamental frequencies of 25 to 30 Hz without neural input or muscular contraction. This strongly suggests that the physical and physiological basis of cat purring involves the same MEAD-based mechanisms as other cat vocalizations (e.g., meows) and most other vertebrate vocalizations but is potentially augmented by AMC.

RESULTS

Vocal production in the cat family Felidae has excited great scientific interest since Richard Owen's classic 1833 demonstration that the structure of the hyoid apparatus underlies the distinction between the Pantherine or "roaring" cats (genus *Panthera*—lions, tigers, etc.) and the Feline or "purring" cats (genus *Felis*—domestic cats and many others).[5,6] More recently, the capacity of the roaring cats to produce loud, low-pitched roars has been shown to depend on the unusual structure of their vocal folds, while their elastic hyoid apparatus and elongated vocal tract leads to lowered formant frequencies.[7–9] In contrast, the production of unusually low-frequency purrs in the purring cats—occurring at alternating phases of egressive and ingressive vocalization (see Figure S1 for an example) —is currently believed to rely entirely upon neural control, specifically neurally driven muscle contractions at the purr rate; i.e., the "active muscle contraction" or AMC hypothesis.[3,10–12]

Here we show that low-frequency phonation in the purring range (20–30 Hz) can readily be elicited in the excised larynges of domestic cats (*Felis sylvestris catus*) in the absence of muscular contraction or neural input. These low-frequency vocal fold vibrations involve a special vocal mode with an unusually long closed quotient, reminiscent of the "vocal fry" register in humans.[13] We suggest that this vibrational regime combines with an unusual and little-studied anatomical specialization—pads within the cat vocal folds—to allow purr-frequency phonation to be driven by the same aerodynamic mechanisms that generate higher-frequency vocalizations like meows, trills, and screams. Our results indicate that the current consensus opinion that cat purring requires AMC was reached prematurely and that the myoelastic aerodynamic (MEAD) theory, combined with an unusual anatomical adaptation, may be sufficient to explain all vocalization types in domestic cats.

Without exception all eight examined larynges were able to produce vibration and sound at or below the f_o range of domestic cat purring, i.e., 25–30 Hz[10,14] (see Figures 1A and S1). Given the lack of neural input in the utilized *ex vivo* excised larynx setup, the observed aerodynamically driven self-sustained oscillation was
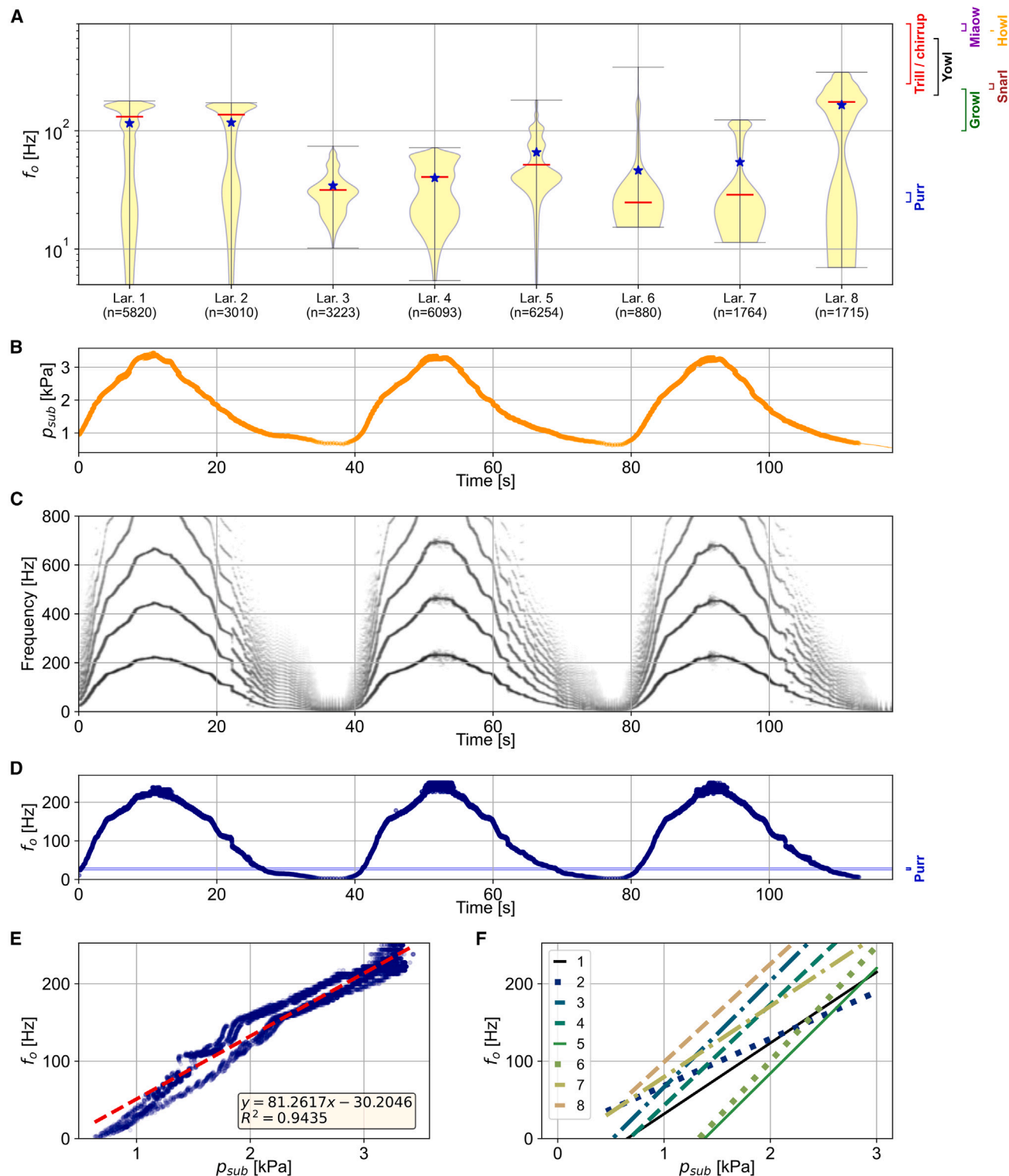
Figure 1. Domestic cat larynges reliably exhibit MEAD-powered self-sustained vocal fold oscillation at purring frequencies

(A–F) Data from all eight investigated larynges.

(A) Violin plots, summarizing the observed f_o values for each larynx, with mean (blue stars) and median (thick red horizontal bars) indicators. The maximum values are indicated as thin black horizontal bars.

(B, C, and D) Subglottal driving pressure (p_{sub}) and resulting acoustic spectrogram and f_o for larynx #1; (E) dependency of f_o on p_{sub} in larynx #1.

(F) Dependency of f_o on p_{sub} in all eight investigated larynges. f_o ranges for different call types are indicated in panels A and D (data from Table 4 in Turner et al.[45]). See also Figures S1–S3.

Current Biology
Report
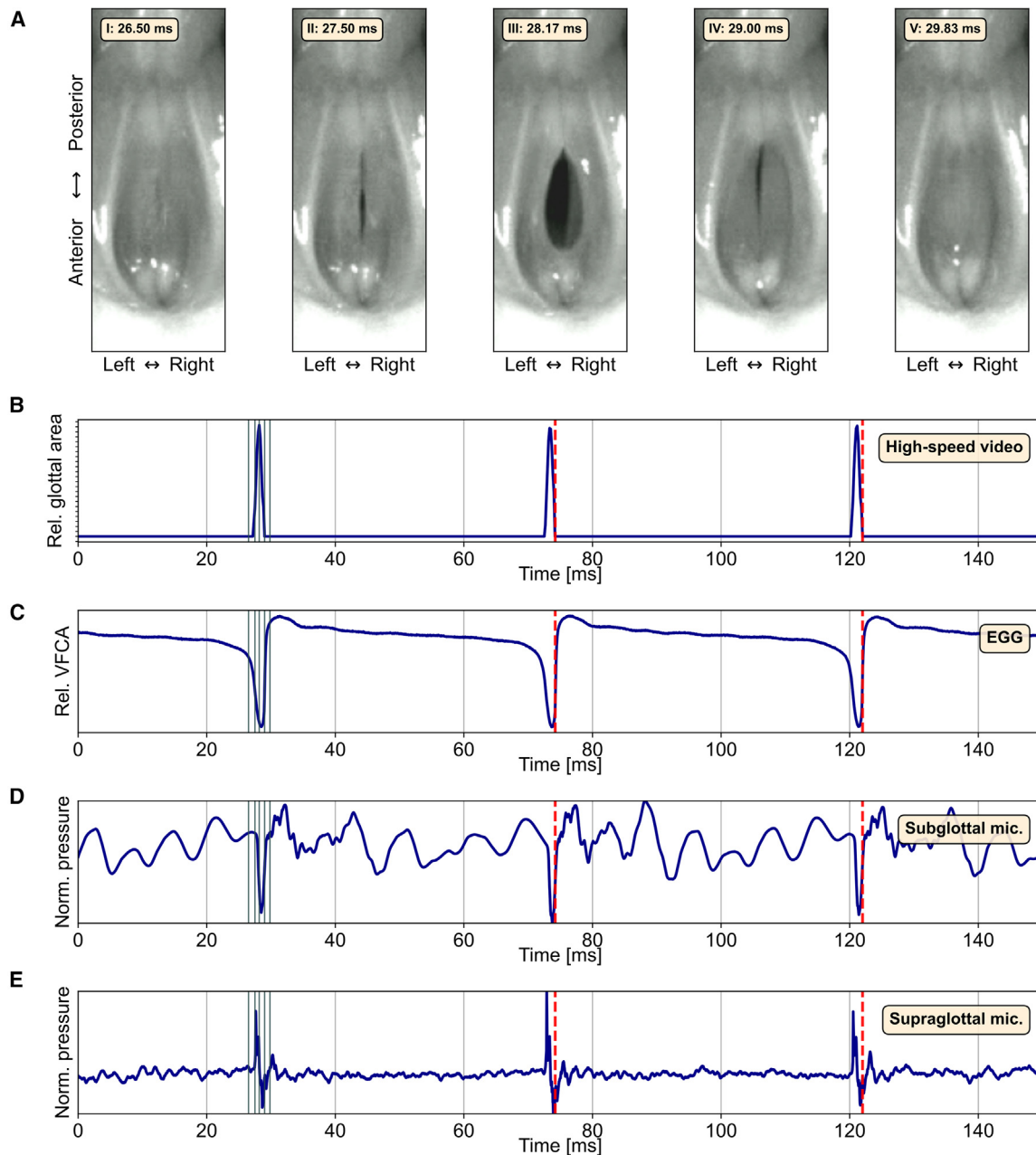
Figure 2. MEAD-driven voice production mechanism in a domestic cat larynx #8 at p_{sub} = 0.8 kPa, $f_o \approx$ 22 Hz
(A) Five HSV frames documenting glottal opening and closure at 6,000 fps.
(B–E) glottal area waveform, electroglottographic (EGG), and acoustic signals. In panels B–E, the gray vertical markers at laryngeal cycle 1 (t = 26.5–29.83 s) indicate the temporal offsets of the five still images from the HSV footage displayed in panel A. The dashed red vertical markers indicate incidents of acoustic excitation for cycles 2 and 3, occurring at the moment of glottal closure. See also Video S1, Datas S1and S2.

governed by the MEAD principle, and an AMC mechanism can be ruled out for the data presented here.

In six of the eight specimens, gradual f_o variation in the ranges of about 15 to 200 Hz (i.e., about 3.7 octaves) occurred, thus creating an f_o continuum between purrs and other stereotypical call types (see Figure 1C and 1D for an example). This suggests that the low-frequency purring-like vibratory phenomena are governed by similar biomechanic and aerodynamic

phenomena as the other, higher-frequency call types of domestic cats. Our data further show that f_o is dependent on the aerodynamic driving pressure, p_{sub} (Figure 1B and 1F), with p_{sub} commensurable with previously reported data for f_o in the range found for purring (25–30 Hz).[3] Additionally, manual elongation of the vocal folds during the experiment (not quantified via the investigative methodology) also had a distinct influence on f_o (increased elongation leading to increased f_o) in all
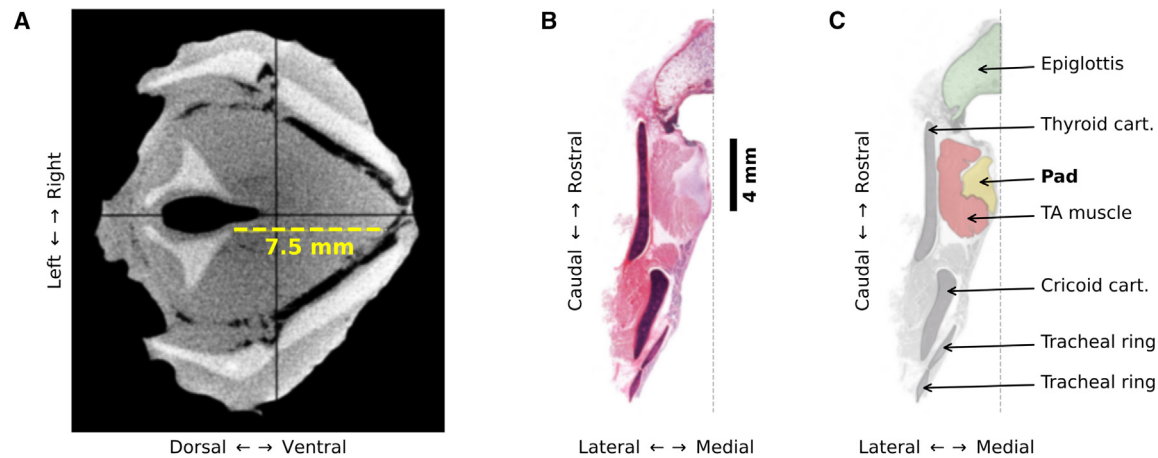
Figure 3. Domestic cat vocal fold anatomy
(A) CT data, transversal cut (the yellow line measures the membranous vocal fold length as 7.5 mm).
(B) Histological representation of larynx #7, coronal cut at the ventro-dorsal center of the vocal folds.
(C) Schematic illustration of image in panel B; the thin dashed vertical lines in panels B and C indicate the glottal midline.

eight larynges, in agreement with previous predictions for mammals more generally.[15]

In all larynges, sound production occurred in synchronicity with cyclic vocal fold vibration and collision. At purring frequencies, the duration of vocal fold contact per oscillatory cycle was surprisingly long, assuming values from 80% to over 95% (Figures 2A–2C). This is comparable to vocal fry phonation in humans,[13] which is found at f_o below 70 Hz.[16,17] The main acoustical excitation—best seen in the supraglottal microphone signal in Figure 2E—is constituted by pressure pulses occurring at the incidents of glottal opening (vocal fold separation) and glottal closure (vocal fold collision). A similar temporal correlation between vocal fold motion—gating the transglottal airflow—and acoustic excitation has been regularly observed in vocalizations relying on the MEAD principle.[18]

DISCUSSION

We propose that the ability to produce self-sustained oscillation at purring-like frequencies is facilitated by a special anatomical adaptation. Rostro-dorsally embedded in the *plica vocalis*, domestic cats have macroscopically visible "pads." These pads run along the inner (glottal) edge of the vocal fold and lack a capsule. They consist of spindle-shaped and star-shaped cells, myxoid tissue, vessels, glycosaminoglycans (mucopolysaccharides), elastic fibers, and sparse collagen fibers (see Figure 3).[4] The pads occur independently of age and sex and can reach a size of up to 4 mm.[4] They are functionally analogous to what has been found in roaring cats[19] in the undivided thyroarytenoid fold.

In analogy to previously presented data,[19] the special tissue composition of the vocal fold pads in domestic cats likely results in a greatly decreased Young's modulus of the most medial portion of the vocal fold. Because oscillation at purring-like frequencies occurs at very low driving pressures, only this most medial portion of the vocal fold contributes to the effective mass in vibration. In such a condition, the biomechanical properties of

the pads take precedence over those of the other vocal fold layers, thus facilitating vibration at the low frequencies observed. A simulation with a simple two-mass model,[20] configured with a greatly reduced spring constant of the model's main mass, supports this assumption (see Figure S3) in agreement with theoretical predictions for roaring cats.[19] The biomechanical functions of the pads are thus functionally analogous to fat structures in toothed whale vocal apparatus that facilitate vocal-fry-like pulse-trains,[21] specialized "switchable" fibrous masses in the túngara frog laryngeal anatomy,[22] and potentially even pathological vocal fold alterations such as Reinke's edema in humans.[23]

From the viewpoint of neural control, electrical brain stimulation results in a clear distinction between purrs and other cat vocalizations, such as meows, growls, and hisses.[24] Moreover, previous evidence suggests the potential co-existence of these fundamentally different call types.[10,25] We therefore do not rule out cyclic neural control during cat purring *in vivo*. However, some issues with the AMC model proposed by Remmers & Gautier[3]—see Herbst et al.[26] for an in-depth discussion—warrant a critical appraisal and revision of the currently accepted purring production hypothesis.

Considering both previous research and the empirical data presented here, we hypothesize that *in vivo* cat purring is facilitated by the co-existence of AMC and MEAD. In particular, we propose that a passive mechanical resonator (the vibrating vocal folds employing the MEAD mechanism) is frequency-entrained to a neuronally driven system (AMC-powered contractions of intrinsic laryngeal muscles). The frequency-entrainment of the coupled oscillator with the passive MEAD component may potentially help to stabilize the periodic oscillation across the phases of egressive vs. ingressive vocalization. This matched active/passive system may also provide energetic benefits, because driving a mechanical resonator at or near its resonant frequency is presumably much more efficient than driving a non-resonant system.

Such a coupled oscillatory system was already briefly discussed by Frazer Sissom et al.[10] These authors dismissed a

Current Biology
Report

CellPress
OPEN ACCESS

Table 1. Overview of domestic cat specimens investigated in this study

Larynx ID	Age [yrs]	Sex	Status	Body Weight [kg]	Body Length [cm]
#1	2	male	not castrated	3.15	53.5
#2	14	female	castrated	2.23	44.7
#3	12.5	male	castrated	2.9	52.5
#4	9	female	not castrated	5.4	48.9
#5	18	female	castrated	1.8	[unknown]
#6	0.5	male	not castrated	1.9	40.3
#7	15	female	castrated	3.1	51.2
#8	16	female	castrated	2	46.7

coupled AMC-MEAD system on the grounds of problematic assumptions of vocal fold mechanics in relation to domestic cats' body mass. In contrast, our data clearly demonstrate that the larynx as a passive mechanical system is indeed able to oscillate at the presumed neuronally induced purring frequencies, at least in egressive vocalization. This is made possible by anatomical adaptation (via the pads embedded in the vocal folds), thus considerably lowering the achievable f_o. Support for such a hypothesis is provided by our data, suggesting an approximate match of the MEAD-driven f_o found *ex vivo* and the observed purring frequencies *in vivo*. Further research will be needed to elucidate the physiological and physical vocal mechanisms that underlie cat purring, but our data unequivocally demonstrate that MEAD-driven vocal fold vibrations at purr frequencies are possible, without neural input or active muscle contraction, and thus that a revised theory of purring is required.

STAR★METHODS

Detailed methods are provided in the online version of this paper and include the following:

- KEY RESOURCES TABLE
- RESOURCE AVAILABILITY
  - Lead contact
  - Materials availability
  - Data and code availability
- EXPERIMENTAL MODEL AND STUDY PARTICIPANT DETAILS
- METHOD DETAILS
  - CT scans
  - Histological analysis
  - Excised larynx preparation
  - Data acquisition
  - Experimental conditions
  - Fundamental frequency (f_o) analysis
  - Signal post-processing
  - Computer simulation of vocal fold vibration
  - Interpretation of subglottal pressure data
- QUANTIFICATION AND STATISTICAL ANALYSIS

SUPPLEMENTAL INFORMATION

Supplemental information can be found online at https://doi.org/10.1016/j.cub.2023.09.014.

REFERENCES

1. van den Berg, J. (1958). Myoelastic-aerodynamic theory of voice production. J. Speech Hear. Res. *1*, 227–244.

2. Titze, I.R. (1980). Comments on the myoelastic - aerodynamic theory of phonation. J. Speech Hear. Res. *23*, 495–510.

3. Remmers, J.E., and Gautier, H. (1972). Neural and mechanical mechanisms of feline purring. Respir. Physiol. *16*, 351–361.

4. Szedenik, K. (2008). Zur Morphologie des Larynx der Hauskatze (*Felis domestica*) (PhD thesis, University of Veterinary Medicine).

5. Owen, R. (1834). On the anatomy of the cheetah. Trans Zool Soc *1*, 129–136.

6. Pocock, R.I. (1916). On the hyoidean apparatus of the lion (*F. leo*) and related species of Felidae. Ann. Mag. Nat. Hist. *18*, 222–229.

7. Peters, G., and Hast, M.H. (1994). Hyoid structure, laryngeal anatomy, and vocalization in felids. Zeitschrift für Säugetierkunde *59*, 87–104.

8. Weissengruber, G.E., Forstenpointner, G., Peters, G., Kübber-Heiss, A., and Fitch, W. (2002). Hyoid apparatus and pharynx in the lion (*Panthera leo*), jaguar (*Panthera onca*), tiger (*Panthera tigris*), cheetah (*Acinonyxjubatus*) and domestic cat (*Felis silvestris f. catus*). J. Anat. *201*, 195–209.

9. Titze, I.R., Fitch, W.T., Hunter, E.J., Alipour, F., Montequin, D., Armstrong, D.L., McGee, J.,, and Walsh, E.J. (2010). Vocal power and pressure-flow relationships in excised tiger larynges. J. Exp. Biol. *213*, 3866–3873.

10. Sissom, D.E.F., Rice, D.A.,, and Peters, G. (1991). How cats purr. The Zoological Society of London *223*, 67–78.

11. Peters, G. (2002). Purring and similar vocalizations in mammals. Mamm Rev. *32*, 245–271.

12. Herbst, C.T., Stoeger, A.S., Frey, R., Lohscheller, J., Titze, I.R., Gumpenberger, M., and Fitch, W.T. (2012). How low can you go? Physical production mechanism of elephant infrasonic vocalizations. Science *337*, 595–599.

CellPress
OPEN ACCESS

Current Biology
Report

13. Hollien, H., and Michel, J.F. (1968). Vocal fry as a phonational register. J. Speech Hear. Res. *11*, 600–604.

14. Schötz, S., and Eklund, R. (2011). A comparative acoustic analysis of purring in four cats. TMH - QPSR *51*, 9–12.

15. Titze, I., Riede, T., and Mau, T. (2016). Predicting achievable fundamental frequency ranges in vocalization across species. PLoS Comput. Biol. *12*, e1004907.

16. Keidar, A. (1983). An acoustic perceptual study of vocal fry, using synthetic stimuli. J. Acoust. Soc. Am. *73*, S3.

17. Titze, I.R. (1988). A framework for the study of vocal registers. J. Voice *2*, 183–194.

18. Švec, J.G., Schutte, H.K., Chen, C.J., and Titze, I.R. (2021). Integrative insights into the myoelastic-aerodynamic theory and acoustics of phonation. Scientific tribute to Donald G. Miller. Journal of Voice *37*, 305–313.

19. Klemuk, S.A., Riede, T., Walsh, E.J., and Titze, I.R. (2011). Adapted to roar: Functional morphology of tiger and lion vocal folds. PLoS One *6*, e27029.

20. Steinecke, I., and Herzel, H. (1995). Bifurcations in an asymmetric vocal fold model. J. Acoust. Soc. Am. *97*, 1874–1884.

21. Madsen, P.T., Siebert, U., and Elemans, C.P.H. (2023). Toothed whales use distinct vocal registers for echolocation and communication. Science *379*, 928–933.

22. Ryan, M.J., and Guerra, M.A. (2014). The mechanism of sound production in túngara frogs and its role in sexual selection and speciation. Curr. Opin. Neurobiol. *28*, 54–59.

23. Zeitels, S.M., Hillman, R.E., Bunting, G.W., and Vaughn, T. (1997). Reinke's edema: Phonatory mechanisms and management strategies. Ann. Otol. Rhinol. Laryngol. *106*, 533–543.

24. de Lanerolle, N.C. (1990). A pontine call site in the domestic cat: behavior and neural pathways. Neuroscience *37*, 201–214.

25. McComb, K., Taylor, A.M., Wilson, C., and Charlton, B.D. (2009). The cry embedded within the purr. Curr. Biol. *19*, R507–R508.

26. Herbst, C.T., Švec, J.G., and Fitch, W.T. (2023). About the voice production mechanism of cat purring – a critical appraisal of Remmers & Gautier (University of Vienna u:scholar repository). https://doi.org/10.25365/phaidra.420.

27. Herbst, C.T., Lohscheller, J., Švec, J.G., Henrich, N., Weissengruber, G., and Fitch, W.T. (2014). Glottal opening and closing events investigated by electroglottography and super-high-speed video recordings. J. Exp. Biol. *217*, 955–963.

28. Garcia, M., Herbst, C.T., Bowling, D.L., Dunn, J.C., and Fitch, W.T. (2017). Acoustic allometry revisited: morphological determinants of fundamental frequency in primate vocal production. Sci. Rep. *7*, 10450–10511.

29. Titze, I.R. (2006). The myoelastic aerodynamic theory of phonation (National Center for Voice and Speech).

30. Švec, J.G., and Granqvist, S. (2018). Tutorial and guidelines on measurement of sound pressure level in voice and speech. J. Speech Lang. Hear. Res. *61*, 441–461.

31. Herbst, C.T. (2020). Electroglottography – an update. J. Voice *34*, 503–526.

32. Herbst, C.T., and Dunn, J.C. (2019). Fundamental frequency estimation of low-quality electroglottographic signals. J. Voice *33*, 401–411.

33. Howard, D.M. (1989). Peak-picking fundamental period estimation for hearing prostheses. J. Acoust. Soc. Am. *86*, 902–910.

34. Smith, J.O., and Serra, X. (1987). PARSHL: an analysis/synthesis program for non-harmonic sounds based on a sinusoidal representation. In Proceedings of the International Computer Music Conference, pp. 290–297.

35. Cranen, B., and Boves, L. (1985). Pressure measurements during speech production using semiconductor miniature pressure transducers: Impact on models for speech production. J. Acoust. Soc. Am. *77*, 1543–1551.

36. Schutte, H.K., and Miller, D.G. (1988). Resonanzspiele der Gesangsstimme in ihren Beziehungen zu supra- und subglottalen Druckverläufen: Konsequenzen für die Stimmbildungstheorie. Folia Phoniatr. *40*, 65–73.

37. Sundberg, J., Scherer, R., Hess, M., Müller, F., and Granqvist, S. (2013). Subglottal pressure oscillations accompanying phonation. J. Voice *27*, 411–421.

38. Alipour, F., and Scherer, R.C. (1995). Pulsatile airflow during phonation: An excised larynx model. J. Acoust. Soc. Am. *97*, 1241–1248.

39. Lehoux, S., Hampala, V., and Švec, J.G. (2019). Development and use of an anechoic subglottal tract for excised larynx experiments. Conference: Models and Analysis of Vocal Emissions for Biomedical Applications - 11th International Workshop.

40. Lehoux, S., Hampala, V., and Švec, J.G. (2021). Subglottal pressure oscillations in anechoic and resonant conditions and their influence on excised larynx phonations. Sci. Rep. *11*, 1–14.

41. Zhao, W., Zhang, C., Frankel, S.H., and Mongeau, L. (2002). Computational aeroacoustics of phonation, part I: Computational methods and sound generation mechanisms. J. Acoust. Soc. Am. *112*, 2134–2146.

42. Zhang, Z., Mongeau, L., and Frankel, S.H. (2002). Experimental verification of the quasi-steady approximation for aerodynamic sound generation by pulsating jets in tubes. J. Acoust. Soc. Am. *112*, 1652–1663.

43. Hunter, J.D. (2007). Matplotlib: A 2D graphics environment. Comput. Sci. Eng. *9*, 90–95.

44. Harris, C.R., Millman, K.J., van der Walt, S.J., Gommers, R., Virtanen, P., Cournapeau, D., Wieser, E., Taylor, J., Berg, S., Smith, N.J., et al. (2020). Array programming with NumPy. Nature *585*, 357–362.

45. Turner, D.C., and Bateson, P.P.G. (2014). The domestic cat: the biology of its behaviour, 3rd edition (Cambridge University Press).

Current Biology
Report

CellPress
OPEN ACCESS

STAR★METHODS

KEY RESOURCES TABLE

REAGENT or RESOURCE	SOURCE	IDENTIFIER
Chemicals, Peptides, and Recombinant Proteins		
Formaldehyde solution 4%, buffered, pH 6.9	Merck KGaA, Darmstadt, Germany	Art. Nr. 1.00496.8350
Software and Algorithms		
Software for time-aligning HSV and physiological voice signals	Herbst, C.T. et al.[27]	
Software for fundamental frequency detection	https://doi.org/10.5281/zenodo.8164521	

RESOURCE AVAILABILITY

Lead contact
Further information and requests for resources and reagents should be directed to and will be fulfilled by the lead contact, Christian T. Herbst (info@christian-herbst.org).

Materials availability
This study did not generate new unique reagents.

Data and code availability
All data reported in this paper will be shared by the lead contact upon request. Any information required to reanalyze the data reported in this paper is available from the lead contact upon request. All original code has been deposited at Zenodo and is publicly available as of the date of publication. DOIs are listed in the key resources table.

EXPERIMENTAL MODEL AND STUDY PARTICIPANT DETAILS

Eight domestic cat larynges (*Felis catus*) were investigated in this study. An overview of the specimens is given in Table 1. The larynges were harvested from animals that had to be euthanised due to terminal disease unrelated to the respiratory tract in veterinary clinics in Vienna, Austria. The animals' owners gave their explicit consent for the larynges to be investigated *postmortem*.

The larynx specimens were extracted immediately *postmortem*. They were immediately flash frozen using liquid nitrogen, and were then stored at -20°C. During the night before the experiment, each larynx was slowly thawed at room temperature.

METHOD DETAILS

CT scans
Larynx #8 was scanned with a XRadia MicroXCT-400 (Carl Zeiss X-ray Microscopy, Pleasanton, CA, USA). The following parameters were used for the scan: Source settings: 40kVp, 200μA (no X-ray Filter used); Detector Assembly: 0.4X; Camera binning: 2; Isotropic voxel size: 41.0238 μm; Exposure time per projection: 3s; Angular increment between projections: 0.25°. No contrast solution was applied to the larynx specimen.

Histological analysis
After *ex vitro* investigation in the excised larynx setup, larynx #7 was fixed in a 4% buffered formaldehyde solution (Art. Nr. 1.00496.8350, Merck KGaA, Darmstadt, Germany) and routinely embedded in paraffin. Several coronal cuts with 4 μm thickness were made. The resulting sections were stained with haematoxylin/eosin and scanned using an Aperio CS2 slide scanner (Leica Microsystems GmbH, Wetzlar, Germany) at a 20× objective magnification.

Excised larynx preparation
The excised larynx setup described previously[12,27,28] was used in this study. At the day of the experiment, each larynx was cleaned, inspected and photographed. After removing excess tissue and all but four tracheal rings, each larynx was mounted on a vertical tube that could supply heated (∼37°C) and humidified (100% humidity) air. Larynx stability was maintained with an adjustable plastic support structure (using LEGO blocks, Billund, Denmark) and 3D-printed plastic mounts. The vocal folds were adducted to a medialized position using prongs that were inserted at the level of the arytenoids, as described by Titze[29, Chapter 1.5.4]. Vocal fold adduction was

manually fine-tuned using a paired set of micromanipulators (Warzhauser MM33, Tamm, Germany). To facilitate acquisition of the electroglottographic (EGG) signal, a set of custom-made copper-plated miniature electrodes was attached to the thyroid cartilage at the level of the vocal folds, with one electrode on each side.

Data acquisition

A number of measurement signals were acquired simultaneously as follows:

The <u>acoustic signal</u> was acquired with a DPA 4061 omnidirectional microphone (DPA Microphones A/S, Alleroed, Denmark), obliquely positioned 8 cm from the vocal folds at an angle of 45°. That signal was calibrated with a NL-52 RION sound pressure level-meter (RION Co., Ltd., Amstelveen, The Netherlands) using a method proposed by Svec & Granqvist.[30] In order to assess the relative inter-cycle acoustic pressure variations within the subglottal tract, a second DPA 4061 microphone was positioned at a level of 15 cm below the vocal folds, aligned flush with the inside wall of the subglottal tract at a perpendicular angle to the subglottal airflow. Both DPA 4061 microphones were pre-amplified using a RME Fireface 800 external sound card (Audio AG, Haimhausen, Germany).

<u>Electroglottographic</u> (EGG) data were acquired with a Glottal Enterprises EG2-PCX2 two-channel electroglottograph (Glottal Enterprises Inc., Syracuse, NY). The EGG signal is proportional to the time-varying relative vocal fold contact area (VFCA).[31] Because the EGG signal provides direct information on laryngeal voice production and is not influenced by acoustic phenomena (thus avoiding potential background noise influences), it is perfectly suited for computing the fundamental frequency (f_o) of the investigated information.[31]

Both the microphone signals and the EGG signal were acquired with a RME Fireface 800 external sound card driven at a sampling frequency of 44100 Hz.

<u>Subglottal pressure</u> (p_{sub}) was measured with a Keller PR-41X pressure sensor (KELLER Druckmesstechnik AG, Winterthur, Switzerland) positioned 32 cm upstream from the vocal folds. Time-averaged <u>glottal airflow</u> data were acquired using an Aerophone II flowhead (F-J Electronics, Vedbaek, Denmark) positioned upstream from the pressure transducer, in combination with a SDP1000-L05 differential pressure transducer (Sensirion AG, Stäfa, Switzerland). The differential pressure transducer was calibrated before the experiment using an Influx A15HS ISS:3 LU11 rotameter (Influx Measurements Ltd. Alresford, UK), resulting in a linear correlation between calibration and measurement data within the range of 0 to 100 L/min (R^2 = 0.999). Pressure and airflow data were acquired with a Labjack U6 Precision USB Multifunction DAQ (LabJack Corporation, Lakewood, CO) at a sampling rate of 1000 Hz.

In larynx #8, <u>high-speed video</u> (HSV) footage of the vibrating vocal folds was acquired with a MotionBLITZ LTR1 portable camera (Mikrotron, Unterschleissheim, Germany). The camera was operated at a frame rate of 6000 frames per second (fps). Illumination was provided by a Cymo 7300.03 300W Xenon Light Source (Cymo, Groningen, The Netherlands).

The three involved systems (the RME Fireface sound card, the LabJack U6 DAQ, and the HSV camera) were <u>synchronized</u> using a custom transistor-transistor-logic (TTL) signal emitted by the LabJack U6 data acquisition card. This TTL signal consisted of pulses of approximately 20 ms duration that encoded the running recording time. The TTL signal was routed through an IC555 timer circuit (having pulse rise time 15 ns) and was simultaneously recorded by all recording devices in dedicated channels. In the HSV camera, the TTL signal was encoded within one pixel in the upper left part of the recorded image data, and was later extracted with custom-built software for time-aligning the camera footage with the other signals. The maximum synchronization error was estimated as $T_\varepsilon \leq$ 166.7 μs [μs], which is the time delay between two consecutive video frames at a video frame rate of 6000 fps. Further details are given in a previous publication.[27]

Experimental conditions

The eight larynges investigated here were subjected to two experimental conditions. In condition (A) the oscillation was driven by subglottal pressure (p_{sub}) that was varied in the range of about 0.3–3 kPa (values varied between larynges). p_{sub} was controlled automatically by gradually opening and closing a magnetic valve in the air supply chain. This valve was voltage-driven through a signal emitted by the LabJack U6 DAQ, controlled by a custom Python software and graphical user interface (GUI) written by CTH. In condition (B), the lowest achievable fundamental frequencies () in each larynx were explored by manually varying p_{sub} (again controlled via the magnetic valve). The human user input for these variations was given via the custom built GUI.

Fundamental frequency (f_o) analysis

Visual inspection of both the acquired EGG time series and their respective narrow-band spectrograms suggested that f_o values as low as 1.3 Hz were to be expected in the data material. A number of f_o detection algorithms[32] had been tested in a preliminary analysis stage. In the end, a custom-built peak-picking algorithm (cf.[33]) operating on the first derivative of the EGG signal (dEGG) was implemented and chosen, because it produced the most robust results even for the extremely low-frequency signals analyzed here. The EGG signals acquired here systematically consisted of waveforms with a very abrupt increase of vocal fold contact area (VFCA) – see Figure S1, panel E. When taking the first derivative of the signal (dEGG), very pronounced positive peaks appeared at the instant of most abrupt VFCA increase (see Figure S1, panel F). These were locally normalized to a maximum positive value of 1, and the incidents were marked where the normalized dEGG signal crossed a heuristically determined threshold of 0.3, that is, 30% of the local maximum. The consecutive threshold crossings $t[i]$ were interpreted as the start offsets of each vibratory cycle. This allowed the computation of each vibratory period as $T[i] = t[i] - t[i-1]$. Because frequency is the multiplicative inverse of period, the equivalent fundamental frequency at the moment of each respective glottal cycle was derived as $f_o [t_{cycle}] = 1 / (T[i])$, where $t_{cycle} = 0.5 (t[i-1] + t[i])$ – see

Current Biology
Report

CellPress
OPEN ACCESS

Signal post-processing

For analysis and illustration purposes (see Figure 2), the acoustic signals were time-shifted to account for their time-delay with respect to the high-speed video footage. The supraglottal and subglottal microphones were positioned at a distance of $d = 8$ cm and $d = 15$ cm from the level of the vocal folds. Considering a speed of sound of $c = 340$ m/s, the time-delay for the signals was computed as $T_{delay} = d / c$, resulting in delay values of 0.206 ms and 0.441 ms for the supraglottal and the subglottal microphone, respectively. These delay values were then converted to sample index offsets as $i_{offset} = -int(round(T_{delay} / fs))$, where $fs = 44100$ Hz was the utilized sampling frequency of the acoustic signals. Note that the delay values were almost negligible with respect to the duration of the glottal cycle, amounting to about half a percent of the period.

Computer simulation of vocal fold vibration

In order to theoretically explore the options of the domestic cat larynx for MEAD-like voice production at purring frequencies, vocal fold vibration was simulated with the two-mass model by Steinecke & Herzel.[20] The model was used in its symmetrical default configuration (see[20] for details and parameter values), but using a vocal fold length of 7.5 mm. When doubling the lower mass and dividing the spring constant of the lower mass by a factor of 5, the model lapsed into periodic oscillation at purring frequencies – see Item S4. As with the *ex vivo* data, f_o was dependent on the sub-glottal driving pressure p_{sub}. Even though the utilized model configuration may not be entirely realistic because the actual biomechanical properties of the domestic cat vocal folds have not been investigated in the course of this study, a crucial insight can be gained from the model behavior: In analogy to what was previously found in roaring cats,[19] it is most likely that the domestic cat's specific vocal fold anatomy supports the generation of low-frequency sounds in the purring range. In particular, we postulate that the presence of the "pads" described in previous work[4] lower the vocal folds' elastic modulus (cf.[19]) in order to support the low oscillatory frequencies observed here.

Interpretation of subglottal pressure data

Analysis of previously published subglottal pressure data, obtained during exhalatory phonation *in vivo*[18,35–37] and *ex vivo*[38–40] suggests that the subglottal pressure (p^{sub}) signal is established by a superposition of the following components.

- (A) a positive peak at the incidence of glottal closure, time-correlated with the acoustical excitation. This peak occurs in *in vivo* data, which is naturally produced with an attached supraglottal vocal tract,[18,35–37] while it is typically not found in excised larynx data.[38–40] Likely, the supraglottal vocal tract *in vivo* helps to establish the shedding of unsteady vortices that is required to establish a dipole sound source.[41,42] An absent – or at least greatly reduced – dipole sound source could partially explain the difference of sound pressure level (SPL)[29] that is observed in excised larynx experiments, lacking a vocal tract.
- (B) a more or less pronounced, but systematically appearing negative "dip" (or pressure drop) which spans the entire open phase and likely has its peak at the moment of maximum air flow (see for instance Figure 2 in Lehoux et al.[40]). This feature can be attributed to negative Bernoulli pressure, which is dependent on the speed of air flow. The phenomenon becomes more apparent and influential when there is a large change of the speed of airflow within the glottal cycle, which is particularly the case when the glottal cycle is characterized by a short open phase (thus explaining the absence of the "dip" in "breathy" voice production with incompletely adducted vocal folds).
- (C) AC (alternating current) oscillations superimposed upon the signal, caused by subglottal vocal tract resonances. These are absent in the anechoic condition – compare Figures 3 and 4 in Lehoux et al.[39]

The *ex vivo* data presented here in Figure 2D is mostly made up of elements B (a very pronounced subglottal pressure drop during the remarkably short open phase) and C (effects of subglottal tract resonances, likely due to the low frequency resonances present in the long tubing system supplying air to the investigated excised larynges). As in data from other excised larynx preparations (cf.[38,39]), component A is not found in our data.

Component B – the pronounced negative "dip" of the subglottal signal in Figure 2D – needs further elaboration. Firstly, because of the remarkably short open phase found in our data, this "dip" could be mistaken for a negative pressure peak, as found in the supraglottal acoustic signal at the incident of glottal closure. However, careful analysis of our data suggests that the negative peak value is not reached during the incident of vocal fold collision, but slightly earlier, about halfway during the open phase. Secondly, the large magnitude of this phenomenon in our data can be explained as follows:

The displayed phonation occurred with an average DC airflow of 0.8 L/min. Because of the high closed quotient of 0.96 (the glottis was closed 96% of the cycle), the air flow had to occur during 4% of the glottal cycle, resulting in an average flow rate of 20 L/min for the "flow phase" of each cycle. At the position of the subglottal microphone, the tracheal tube had a diameter of 24 mm, and thus a cross-sectional area of 4.524×10^{-6} m². Dividing the flow volume by the cross-sectional area results in a flow speed of $v = 0.73683$ ms^{-1}. The air density of humidified (100%), heated air (35°C) is $\rho = 1.14566$ kg m^{-3}. Applying Bernoulli's formula

Current Biology
Report

$q = 0.5\rho v^2$ results in an estimated pressure drop of $q = 0.311$ Pa, i.e., the equivalent of a sound level of 84 dB. Due to a technical issue, the subglottal pressure signal was not calibrated, and therefore, unfortunately, a direct comparison of subglottal sound pressure and Bernoulli pressure was not possible.

QUANTIFICATION AND STATISTICAL ANALYSIS

The violin plots shown in Figure 1, panel A and Figure S1, panel C were generated with the matplotlib.pyplot.violinplot function contained in the open source matplotlib software framework for the Python programming language.[43] These plots contain information on group mean values (blue stars), median values (red horizontal lines) and extrema (minimum and maximum values of each group, indicated as thin black horizontal lines). The n values in Figure 1, panel A, indicate fundamental frequency data points extracted from the collected signals (per larynx) every 5 ms. The violin plots in Figure S1, panel C indicate fundamental frequency data points extracted from the collected signals (exhalatory and inhalatory purring phases) every 50 ms.

The first order linear regression fits shown in Figure 1 panels E and F and Figure S3 panel D were generated with the numpy.polyfit function contained in the numpy module for the Python programming language.[44]